Performance Evaluation of High Sensitivity GNSS Techniques in Indoor, Urban and Space Environments

E. Domínguez, A. Pousinho, P. Boto, *GMV, Spain*;
D. Gómez-Casco, S. Locubiche-Serra, G. Seco-Granados, J. A. López-Salcedo, *UAB, Spain*;
H. Fragner, F. Zangerl, *RUAG, Austria*;
O. Peña, *Tecnalia, Spain*;
D. Jiménez-Baños, *European Space Agency, The Netherlands*

BIOGRAPHY

Enrique Domínguez received a M.Sc. degree in Telecommunications Engineering in 2000 and a Master in Space Technologies in 2009, both from the Polytechnic University of Madrid. He joined GMV in 2000 working first in the development of EGNOS and Galileo and since 2009 in GNSS software receivers, multi-sensor fusion algorithms and integrity algorithms.

André Pousinho received his M.Sc. in GNSS from the Technical University of Munich, Germany. He joined GMV in 2014 and he is working on GNSS receiver technologies and signal processing techniques.

Pedro Boto holds a M.Sc. in Aerospace Engineering from Instituto Superior Técnico of Lisbon, Portugal. He joined GMV in 2014 being involved in several projects related with GNSS receiver technologies and signal processing techniques.

David Gómez Casco received the B.Sc. and M.Sc in telecommunication engineering in 2012 and 2014, respectively, from Universitat Autònoma de Barcelona (UAB). In December 2014 he started the PhD studies at the SPCOMNAV group, also involved in the research of new techniques of signal acquisition for GNSS receivers in conditions of weak signal reception.

Sergi Locubiche-Serra received the M.Sc. degree in Telecommunication Engineering in 2014 from Universitat Autònoma de Barcelona (UAB). He is currently working towards the Ph.D. at the SPCOMNAV group. His research interests include statistical signal processing and Kalman filter theory applied to GNSS signal tracking.

Gonzalo Seco-Granados holds a PhD degree from Univ. Politecnica de Catalunya (UPC) and an MBA from IESE, Universidad de Navarra. Since 2006, he is associate prof. at the Dept of Telecom. Eng. of UAB and head of the SPCOMNAV group.

José A. López-Salcedo received the M.Sc. and Ph.D. degrees in Telecommunication Engineering in 2001 and 2007 from UPC. He joined UAB and the SPCOMNAV group as an assistant prof. in 2006, and since 2013 he is an associate prof.

Heinrich Fragner received his M.Sc. degree in Electrical Engineering from the Vienna University of Technology in 1997, and his Ph.D. in Physics from the University of Vienna in 2005. He worked on the design and implementation of signal processing algorithms for Radar and communication systems. Since 2009 he works as project manager for development projects of on-board GNSS receivers at RUAG GmbH.

Franz Zangerl received his M.Sc in Electrical Engineering from the Technical University of Vienna in 1990. He is leader of the processing system group at RUAG GmbH. Since 1997 is working as system engineer in the area of GNSS receivers for space applications.

Orlando Peña received his Telecom Engineer Degree in 1992, in the University of Basc Country (Spain), MPhil by Research at University of Bradford (UK) in 1995. He joined Tecnalia in 2001, and has been working in GNSS RF-FE for more than five years.

David Jiménez-Baños holds MSc. degrees in Telecommunications Engineering and Information and Communication Technologies from the Universitat Politècnica de Catalunya. Since 2006 he has been working at the Radio Navigation Systems and Techniques section of ESA/ESTEC, The Netherlands. His main areas of work have been on GNSS signal processing for indoor and AOCS applications in GEO and higher orbits, SBAS systems, and GNSS simulation tools for receiver performance evaluation.

ABSTRACT

Conventional GNSS receivers have problems in weak signal environments making it difficult to provide GNSS position fixes, and this constitutes one of the bottlenecks in the extension of location services in indoor and dense urban conditions. Besides the signal attenuation, the main

limitations faced in such environments are due to the complex propagation of the GNSS signals (multipath) and due to the different attenuation of the signals coming from different satellites, which may cause cross-correlation peaks to be on the order or even higher than the true autocorrelation one, also known as near-far (NF) problem.

These limitations have led to four main groups of strategies with all sorts of combinations of them in the form of hybridized receivers:

- High-sensitivity GNSS receivers,
- Positioning using sensors (inertial, pressure, optical…),
- Positioning using telecom/wireless networks,
- GNSS pseudolites.

High-sensitivity GNSS receivers are the stand-alone approach to cope with the weak signal problem, these receivers are designed to exploit the little energy that reaches them, which in general terms has been translated into the use of open-loop or snapshot architectures that dwell on the incoming signal for extremely long periods (compared to conventional GNSS receivers). By means of long non-coherent integration, they can achieve low sensitivity, and avoid the effects of bit transitions and clock drifts [1].

The idea of High-sensitivity GNSS receivers is neither new nor original. In most cases previous studies have focused on weak signal acquisition. A thorough review of the indoor challenges and techniques for weak signal acquisition can be found in [2]. However, optimal weak signal tracking and transition from acquisition to tracking has not been sufficiently addressed, some examples can be found in [3] and [4], but in this work the focus was not put into high-sensitivity techniques. In [5] while tracking techniques have been considered, only the urban case (CN0>20 dBHz) with a focus on multipath estimation has been studied. Further studies on high-sensitivity tracking techniques and characterization of the loops in the vicinity of their threshold are needed.

Regarding the multipath problem several strategies can be found in literature to mitigate its effects [6], [7]. Some novel works have shown that it can be possible to use this effect, usually considered adverse, to improve the receiver positioning in weak signal environments [8].

With respect to the near-far problem, inherent protection by the use of spreading codes with cross-correlation margins on the order of 24-28 dB may not be sufficient in the indoor case. Some techniques mainly based in the existing background in multiuser detection techniques for CDMA wireless communications are reviewed in [2]. However, research onto low-complexity near-far mitigation techniques is still an open area and needs further study. Longer spreading codes in modernized GNSS signals (including Galileo) provide better protection against near-far but this also brings more complex processing. Trading-off the advantages gained by the increased protection versus the added complexity is also an open research line.

Moreover, the usage of high-sensitivity techniques is not only restricted to the urban/indoor case other use cases such as space applications (HEO/LEO orbits) need these type of receiver architectures. Multipath, the propagation channel, and user dynamics are vastly different but the signal attenuation can be similar to the indoor case. Therefore modified techniques based on the extensive works already done for the indoor/urban case need to be studied and tailored to this use case.

INTRODUCTION

The work presented in this paper has been developed within the frame of the High-Sensitivity Receivers (HISENS) project, which was developed by a consortium including GMV, UAB, RUAG and Tecnalia and funded by the European Space Agency.

The purpose is to perform an extensive evaluation of the leading edge high sensitivity GNSS signal processing techniques in the following use cases:

- Static Indoor
- Dynamic Indoor
- Urban Canyon
- Space Applications

Firstly, the paper provides a performance assessment of the different high-sensitivity techniques in order to select the most promising ones. The analysed techniques include:

- Open-loop / Snapshot Techniques (Acquisition):
    - Advanced correlation techniques
    - NF Detection Techniques
    - NF Mitigation Technique
    - Multipath Detection
- Closed-loop Techniques (Tracking).

In order to further investigate and evaluate the performances of the selected high-sensitivity techniques a test campaign was carried out covering the four different use cases, each one being tested with simulated (using a SPIRENT simulator) and real data, except for the space applications case which was only tested with the simulator. The RF samples were collected with the Proof of Concept platform developed within the HISENS project, which is based on Tecnalia's HORUS3000 dual-frequency Front-End, a flexible and fully user controlled GNSS RF-FE configured to record samples in L1/E1 and L5/E5a bands.

The paper starts assessing the performance of the different known GNSS signal processing techniques, selecting the most suitable ones to be tested in each use case with the simulated and real data. Then the platform used to collect the RF samples is described along with the configuration of the simulated and real tests. Finally, the results obtained for each use case are provided comparing the performance of the different techniques also assessing the impact on the positioning and timing accuracy.

Weak signal conditions are certainly the main obstacle for the ubiquitous operation of GNSS receivers, particularly in indoor/urban environments. Problems arise when GNSS receivers are moving indoors, since the severe attenuation makes it very difficult to detect/track the received signals.

Two families of **high sensitivity signal processing techniques** were evaluated:

- Enhanced Snapshot Processing Techniques (Open-loop)
- Innovative Closed-loop Techniques

ENHANCED SNAPSHOT PROCESSING TECHNIQUES

The main adverse effects on the detection of weak signal conditions are the following:

a) Signals broadcast from satellites in view are not detected by the GNSS receiver, or conversely, a satellite not in view is declared to be present.
b) Signals broadcast from satellites in view are detected, but the accuracy of the measurement has a huge error.

For this reason, the presence of weak signal conditions is a dramatic challenge on the signal processing algorithms. It is clear that to be eventually able to detect weak signals, there is no choice but to accumulate the received signal during long observation intervals, but coherent integration alone may not yield a sufficient signal to-noise ratio to permit a reliable decision in the detection of satellites.

When the received signal arrives highly attenuated, it is necessary to dramatically increase the integration time. In that case, Post-Detection Integration (PDI) techniques are applied. In fact, the correlation extends to non-coherent (using the squared absolute value, conventionally) to prevent the residual Doppler error from accumulating and cancelling the signal. If this happened, the total integration would decrease to zero instead of gradually increase, which would not allow us to take a reliable decision in the detection of the satellites. Increasing the dwell time in two-dimensional frequency-time hypothesis testing is, in practical terms, one of the most effective ways for Assisted Global Navigation Satellite Systems and GNSS receivers to achieve higher sensitivity [9].

This is the so-called High Sensitive GNSS principle, and it is based on improving the receiver sensitivity through the use of extended correlations combining coherent and non-coherent integration. More specifically, first coherent correlation is employed, and then the outputs of several coherent correlations are non-coherently accumulated from the nonlinear operations. Due to the complexity caused by the widely implemented method of FFT-based acquisition, a great challenge is how to reduce the complexity of the overall system [10]. The complexity of the procedure can be reduced by using "double-FFT algorithm". It allows us to efficiently carry out the time-frequency search using almost exclusively FFT operations [11].

The question is that is not clear which we want to clarify with this study is the method that should be used to perform non-coherent correlation with best performance. Different papers are focused on this problem and they have proposed different techniques or strategies in order to improve the sensitivity of non-coherent correlation.

Double-FFT Method

Efficient acquisition can be implemented through the "double-FFT method" [11] [12] [13] [14]. Such a method is an evolution of the snapshot-based processing in [15]. It assumes that blocks of samples of two codes durations are stacked into matrix form. Then, two FFT operations are applied to this matrix. The first one is done to carry out the convolution with the local code. The second one is done to jointly estimate the Doppler and the secondary code shift.

Figure 1 is the graphical representation of the fundamentals of this method. It can be seen how the basic data matrix (**M**) is constructed. This matrix will be the core structure for the delay and Doppler search explained later.

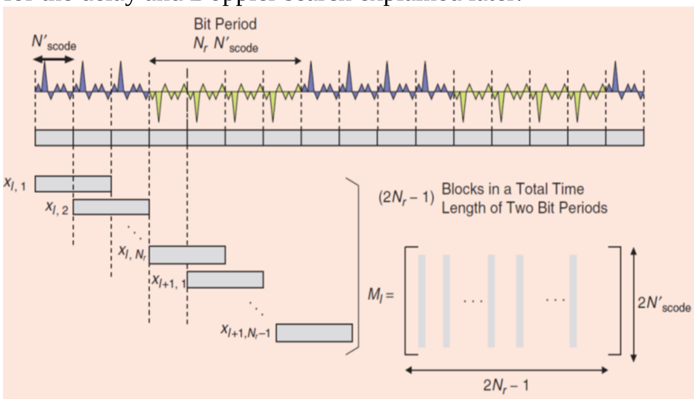

Figure 1 Schematic representation of the signal samples to be considered for the double FFT method

The length of the secondary code is indicated by N_r , the number of code chips by N_c, and the number of samples per chip by N_{sc}. Note that the figure above supposes that data signals and all-ones secondary codes are used. However, the procedure can be adapted for pilot components and a different secondary code. For instance, the length of the secondary code of the E1C signal is 25 bits ('0011100000001010110110010') can play more or less the role of the sequence of 20 PRN codes within a bit of the GPS L1 C/A signal, which was the one originally assumed in the double-FFT method.

Once the double data blocks have been stacked into matrix $\mathbf{M}$, fast convolution is achieved by performing the following operation $\mathbf{M}_{fast\ conv} = \mathbf{F}^{\mathbf{H}}[(\mathbf{F}\cdot\mathbf{M}) \otimes (\mathbf{F}\cdot\mathbf{C})]$, with $\mathbf{F}$ the discrete Fourier matrix, $\mathbf{C}$ the local code of the E1C signal matrix (assuming e.g. that we are processing the Galileo E1 pilot) with replicate columns, $\otimes$ the Schur-

Hadamard product, and $\mathbf{F}^{\mathbf{H}}$ the inverse discrete Fourier matrix. In practice, the efficient implementation of this equation involves the substitution of the DFT transform by the FFT.

Once fast convolution is performed, a sliding submatrix selects some of the terms in matrix **M** as shown in Figure 2, and takes the FFT of each row. The dimensions of this sliding matrix are $(N_r N_{sc} \mathrm{x} N_r)$ so that a total of $N_r N_{sc}$ FFT are calculated by zero-padding the N_r signal samples until the required frequency resolution to detect Doppler is achieved. The size of the zero-padded FFT is to be referred as N_{FFT}.

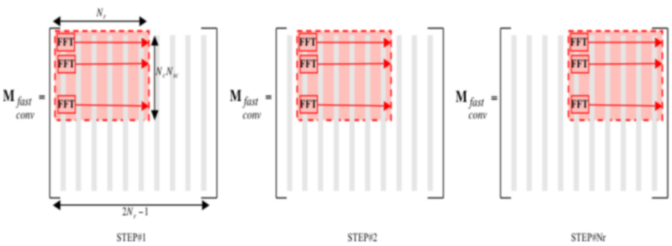

Figure 2 Iterations for the code delay and Doppler search

The results of the FFT operations with the rows of the data matrix are stored in an acquisition hypercube whose dimensions are equal to $(N_r N_{sc} \mathrm{x} N_{FFT} \mathrm{x} N_r)$. To extend the integration time and avoid unknown symbol transitions, non-coherent integration is performed with the values contained within the hypercube. The final step after moving the sliding matrix up to *Nr* positions is to feed the hypercube to the threshold decision block to detect the signal and estimate the code delay and the Doppler frequency.

Advanced Correlation Techniques

Different techniques of non-coherent integration were analysed. The main ones are briefly described hereafter:

Non-coherent Post-Detection Integration (**NPDI**) is the technique most commonly used in the non-coherent integration, it sums the squared absolute values of the coherent correlations [16].

$$Z_{NPDI}(\tau, f_D) = \sum_{n=1}^{N_{nc}} |R_n(\tau, f_D)|^2 \quad (1)$$

Where N_{nc} is the number of non-coherent integrations ($n = 1, \ldots, N_{nc}$) and $R_n(\tau, f_D)$ are outputs of the n coherent integration.

Alternatively, the Differential Post-Detection Integration (**DPDI**) [17] can be used. It is expressed as:

$$Z_{DPDI}(\tau, f_D) = \left|\sum_{n=1}^{N_{nc}-1} R_n(\tau, f_D) R_{n-1}^*(\tau, f_D)\right| \quad (2)$$

The basis of the DPDI is that the noise components of two coherent correlations are uncorrelated with each other, while the signal components are strongly correlated. The lack of correlation between the two consecutive noises allows us to reduce the effect of squaring the noise. Thereby, DPDI provides a sensitivity gain over NPDI.

Another variant of DPDI is the Different Differential (**DD**). It has the same structure as the DPDI, but it contains the absolute value within the summation:

$$Z_{DD}(\tau, f_D) = \sum_{n=1}^{N_{nc}-1} |R_n(\tau, f_D) R_{n-1}^*(\tau, f_D)| \quad (3)$$

Another alternative is the Generalized Post-Detection Integration Truncated (**GPDIT**) [18] and it can be expressed as:

$$Z_{GPDIT}(\tau, f_D) = \sum_{n=1}^{N_{nc}} |R_n(\tau, f_D)|^2 + 2\left|\sum_{n=2}^{N_{nc}} R_n(\tau, f_D) R_{n-1}^*(\tau, f_D)\right| \quad (4)$$

The key point of this technique is that combines the term corresponding to NPDI with the one corresponding to DPDI, which could lead to a better detection probability than NPDI and DPDI.

Another practical approach based on the Generalized Post-Detection Integration was proposed in [19]. This method is so-called fractional **GPDI** and it is the same as $Z_{GPDIT}(\tau, f_D)$, but with some terms raised to a different exponent.

$$Z_{GPDIF}(\tau, f_D) = \sum_{n=1}^{N_{nc}} |R_n(\tau, f_D)|^p + 2\left|\sum_{n=2}^{N_{nc}} R_n(\tau, f_D) R_{n-1}^*(\tau, f_D)\right|^{p/2} \quad (5)$$

An additional method has been proposed in recent years [20]. The main idea behind this method is that it combines the term corresponding to NPDI with a new term. This new term is referred to as squaring detector (**SD**) and it consist of summing the squared values of the outputs of the coherent integrator. The method is defined by:

$$Z_{NPDI+SD}(\tau, f_D) = \sum_{n=1}^{N_{nc}} |R_n(\tau, f_D)|^2 + \left|\sum_{n=1}^{N_{nc}} R_n(\tau, f_D)^2\right| \quad (6)$$

The last studied method, to which we refer as **GPDITSD**, is a novel contribution and is the result of putting together terms of the GPDIT with the SD:

$$Z_{GPDITSD}(\tau, f_D) = \sum_{n=1}^{N_{nc}} |R_n(\tau, f_D)|^2 + 2\left|\sum_{n=1}^{N_{nc}-1} R_n(\tau, f_D) R_{n-1}^*(\tau, f_D)\right| + \left|\sum_{n=1}^{N_{nc}} R_n(\tau, f_D)^2\right| \quad (7)$$

In order to compare these techniques a wide number of simulations were performed testing the Galileo E1 signal for different C/N0 values (10, 12 and 17 dBHz) and different values of coherent integration: 100ms, 500ms and 1000ms (each one tested for different number of non-coherent integrations). Moreover, two types of simulations were employed, besides both include complex additive Gaussian white noise, the first set does not include phase noise while the second includes the phase noise due to the oscillator, which was generated for three different kind of clocks: Chip Scale Atomic Clocks (CSAC), Temperature

Compensated Crystal Oscillator (TCXO) and Oven-Controlled Crystal Oscillator (OCXO). The conclusions of the analysis are presented hereafter.

Without Phase Noise:

When the Doppler frequency error is 0 Hz GPDITSD has the best performance in terms of probability of detection, regardless of the number of non-coherent integrations. Comparing the performance of the methods formed by one term (NPDI, DPDI and SD), when the number of non-coherent integrations is greater than 5, DPDI has the best performance, and when it is smaller than 5 SD has the best performance.

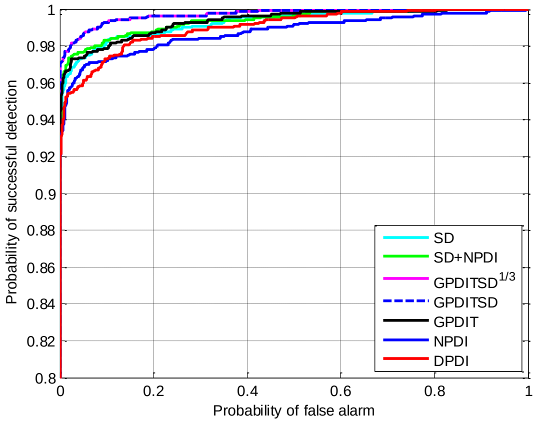

Figure 3 ROC curves for C/N0=10 dBHz, $T_{Coherent}$=1000ms, N_{nc}= 4, and freq. error 0 Hz

However, when the Doppler frequency error is a uniform random variable of ±50Hz, GPDIT has the best performance in terms of probability of detection, regardless of the number of non-coherent integrations, while SD method suffers a significant degradation. Hence, GPDIT outperforms GPDITSD. Comparing the performance of the methods formed by one term, the SD method suffers a significant degradation being worse than the others, and when the number of non-coherent integration is greater than 5, DPDI outperforms NPDI. However, when the number of non-coherent is smaller, the performance of the NPDI and DPDI tends to be the same.

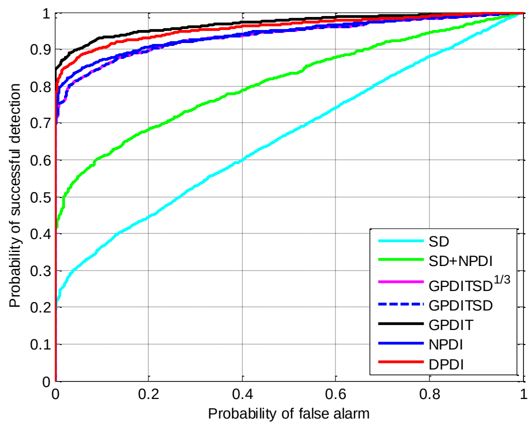

Figure 4 ROC curves for C/N0=10 dBHz, $T_{Coherent}$=1000ms, N_{nc}= 4, and freq. error ±50Hz

With Phase Noise:

The phase noise error introduced by the GNSS receiver clock limits the duration of the coherent integration due to the de-coherence of the carrier during long intervals. The clock error can be modelled and generated using a 2-state system:

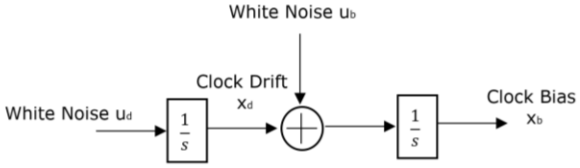

Figure 5 Clock Error Modelling

$$u_b = \sqrt{\frac{S_f}{\Delta T}} N(0,1) \qquad S_f = \frac{h_0}{2} \tag{8}$$

$$u_d = \sqrt{\frac{S_g}{\Delta T}} N(0,1) \qquad S_g = 2\pi^2 h_{-2} \tag{9}$$

Clock Type	h_0 [s]	h_{-2} [s]
TCXO	9.43e-20	3.8e-21
CSAC	7.2e-21	2.7e-27
OCXO	**3.4e-22**	**1.3e-24**

Table 1 White frequency noise and random walk frequency noise clock parameters

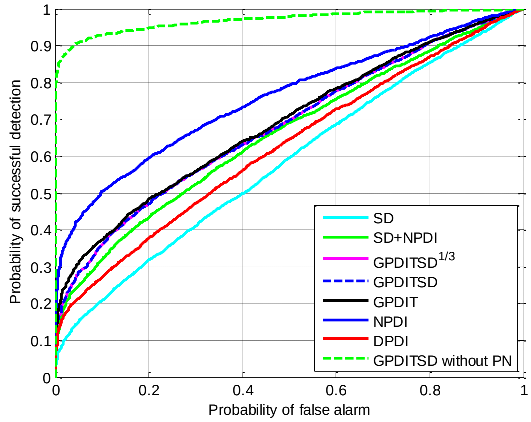

Figure 6 ROC curves for C/N0=12 dBHz, $T_{Coherent}$=500ms, N_{nc}=4, freq. error 0Hz — TCXO

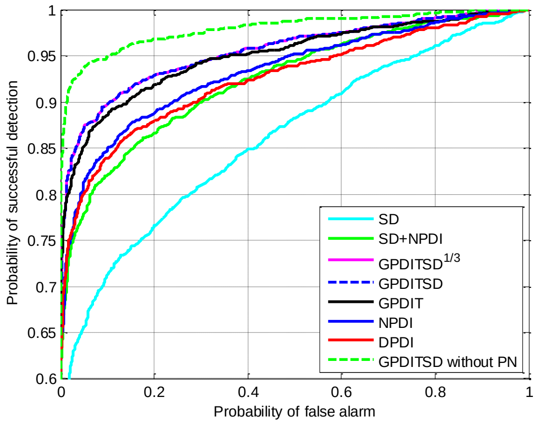

Figure 7 ROC curves for C/N0=12 dBHz, $T_{Coherent}$=500ms, N_{nc}=4, freq. error 0Hz — CSAC

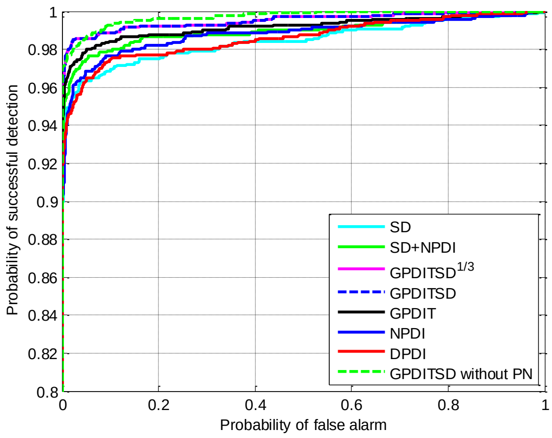

Figure 8 ROC curves for C/N0=10 dBHz, $T_{Coherent}$=1000ms, N_{nc}=4, freq. error 0Hz — OCXO

The performances of the correlation techniques have been analysed for three types of clocks (see Table 1):

- TCXO: can be used to integrate up to 100 ms coherently, with a small degradation of the different correlation methods. However, when coherent integration time is 500ms, it is not possible to satisfactorily detect the signal.
- CSAC: can be used up to 500 ms of coherent integration, but the performance of the methods has a slight degradation at 500 ms. Integrating 1000 ms coherently, the methods show a considerable degradation.
- OCXO: can be perfectly used to integrate 1000ms. The performance of the methods is very similar to the case without the phase noise.

To conclude, the best option for high-sensitivity receivers it to use a medium-quality OCXO clock

Near-Far

The near-far effect (or MAI, *Multiple-Access Interference*) is defined as the condition in which a receiver is affected by a strong signal that hampers the detection of a weaker signal [21]. It is very common in cellular wireless mobile communication systems, and it is particularly relevant in CDMA spread-spectrum communication systems, such as GNSS systems like GPS and Galileo.

The origin of the near-far effect lies in the different attenuation losses incurred by the different propagation paths caused by the presence of different obstacles that the signals coming from the satellites have to pass through.

Two different problems at signal processing level regarding near-far were analysed:

- **Near-far detection**: discriminating between the correlation peaks corresponding to the desired signal and cross-correlation peaks caused by strong interfering signals.
- **Near-far mitigation**: suppress strong interfering signals, so that the weaker desired ones can be acquired afterwards.

Near-Far Detection

The use of spreading codes provides the acquisition process with some inherent robustness against near-far, meaning that the correlation output is not affected by near-far when it is present with an NFR of up to a limited value. GPS L1 C/A and Galileo E1 codes present a cross-correlation protection of about 24dB and 27-28dB respectively for a zero Doppler shift, whereas the protection may decrease by 3-4 dB for any non-zero Doppler shift [22]. However, in indoor environments, urban canyons or space applications the near-far ratio can reach 25-30dB easily and the inherent robustness of GNSS signals may not be enough to withstand the near-far effect. In these situations, the use of near-far detectors is recommended.

When a received satellite is affected by the near-far effect, the correlation output contains the contribution of the desired signal, and also the interference contribution due to non-zero cross-correlation between spreading codes. Thus, the objective of near-far detection techniques is to determine whether a satellite is affected by near-far or not by analysing if the peaks of the correlation output correspond to a weak real weak signal or are caused by a strong interfering signal.

In single-snapshot near-far detection techniques, a statistical hypothesis testing is employed to distinguish between the scenario where near-far is present (also known as the *H1* condition) and the scenario with near-far absent (*H0* condition), as an attempt to exploit the differences in the statistics at the correlation output in *H0* and *H1*:

- When near-far is absent, the correlation output excluding the region surrounding the main peak is dominated by thermal noise. In this case, the squared samples of the correlator output will follow a χ^2 distribution with $2N_{nc}$ degrees of freedom, standing N_{nc} for the number of non-coherent integrations.
- When near-far is present, the correlation output is dominated by the cross-correlation between the strong interfering signal and the code replica of the signal to be acquired. In this case, the statistical distribution of the squared correlator output differs from a χ^2 distribution.

The following near-far detectors were analysed:

- Chi-Square Goodness Of Fit (GOF): is a hypothesis testing technique [23] checking whether the squared samples of the correlator follow a χ^2 distribution.
- Kullback-Leibler (KL) divergence: is another method to quantify the distance to a χ^2 distribution of the squared samples of the correlation output.
- Threshold crossings: tackles on the different statistics of the squared cross-correlation samples in the presence and in the absence of near-far accounting for the number of threshold crossings to a given threshold [24].

- Ratio between two largest correlation peaks: looks at the ratio in power of the received signals [25]. It differs from the previous ones in the fact that it involves all the correlation output samples, including the main peak, whereas the previous approaches exclude the main peak and its surrounding area. In this technique, the decision on near-far detection is carried out by looking at the ratio between the two largest correlation peaks of the correlation output.

The following conclusions can be drawn.

- NFR 24dB: near-far is detected, starting with probabilities of around 25% for all techniques except for the peaks ratio detector, with a probability of 20%. The peaks ratio detector shows the worst performance for all probabilities of false alarm.
  On the other hand, for a probability of false alarm of up to 50%, the threshold crossings detector outperforms the rest of techniques. The chi-square GOF and the KL distance show a similar performance.

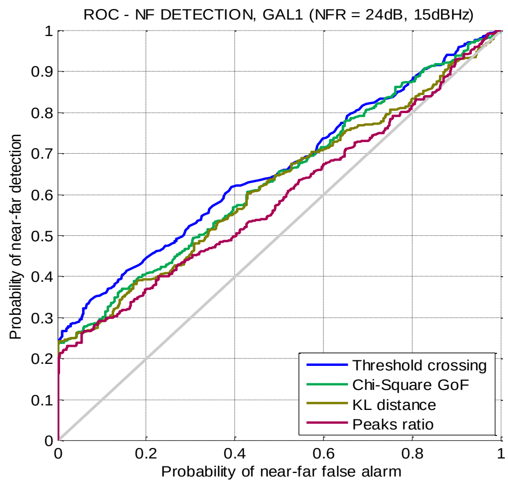

Figure 9 Comparison of NF detection techniques - ROC curves for NFR 24 dB

- NFR 26dB: all techniques show a similar performance, except for the peaks ratio detector. Whereas the former group starts with a detection probability of more than 60%, the latter starts at 60% and never reaches the others. For a probability of false alarm of up to 15-20% the rest of the techniques perform similarly, but for more than 20%, the threshold crossings detector is fairly outperformed by the chi-square GOF and the KL divergence.

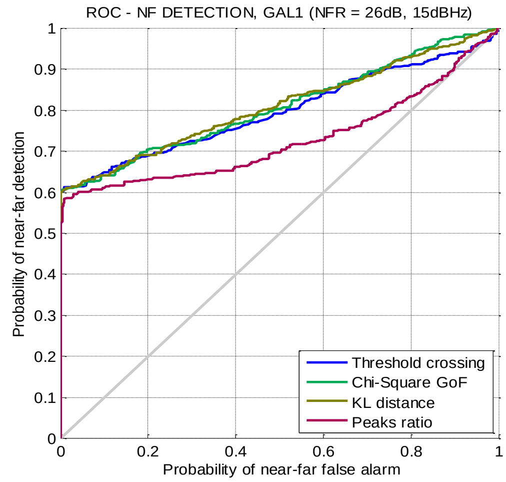

Figure 10 Comparison of NF detection techniques - ROC curves for NFR 26 dB

- NFR 28dB: all techniques show a similar performance, except again for the peaks ratio detector. Whereas the former group starts with a probability of near-far detection of more than 90%, the latter starts at 80% and never reaches the others.

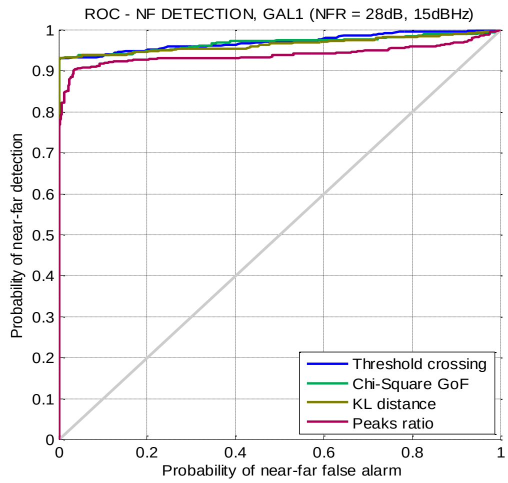

Figure 11 Comparison of NF detection techniques - ROC curves for NFR 28 dB

- NFR 30dB: all techniques (except for the peaks ratio detector) are capable of detecting near-far with a probability close to 100% for a probability of false alarm of 0.24%.

The most critical value of NFR is 24dB, since it is the limit between the inherent protection of spreading codes and near-far detection when the inherent protection fails.

Near-Far Mitigation

Once the near-far interference is detected during the acquisition process of a weak signal coming from a given satellite, near-far mitigation techniques can be applied. They aim is to suppress the strong interfering signals so that such weak desired signals could be acquired afterwards by means of a standard acquisition process.

Multiuser detection (MUD) technology is widely used to deal with the near-far problem, and its application to CDMA systems constitutes the main background for near-far mitigation in GNSS. Near-far mitigation techniques are categorized into two main groups:

- <u>Linear multiuser detectors</u> [26] are claimed to be efficient strategies in decreasing the MAI effects in GPS receivers. Nonetheless, not only do they require the cross-correlation matrix to be calculated but also its inverse, which may translate into a high computational burden. Besides, parameters from all the active users in the system also need to be estimated, including the message data, and furthermore the noise is likely to be enhanced throughout the process [27].
- <u>Cancellation techniques</u>; a good overview of which is found in [28]. They are attractive to near-far mitigation in high-sensitivity GNSS receivers, since they have advantages of low computational complexity and easy implementation. They can be classified in two main categories:
  - Interference cancellation techniques: strong signals are identified and then directly subtracted from the received input signal prior to the correlation of the weaker one [29]. This group of techniques is sometimes also referred to as soft near-far mitigation techniques, mainly comprising successive (SIC) [25] or parallel (PIC) [30] interference cancellation techniques. [28] states that PIC provides better performance when all the strong signals have similar signal levels, whereas SIC outperforms for different strong signal levels.
  - Subspace projection methods: the strong interfering signals are directly suppressed form the received input signal by using different algorithms based on projection operations. Subspace projection techniques are sometimes also be referred to as hard near-far mitigation techniques:
    - Subspace projection technique: the objective is to obtain a new signal in which the contribution of the strong signals has been cancelled, this is achieved by computing the projection of the total input signal onto the strong signals subspace [31]. This projection requires the knowledge of the strong signals amplitude, code delay and Doppler frequency ([32] proves that the projection operator actually does not depend on the carrier phase estimates).
    - Adaptive code replica techniques: consist in building a different code that rejects the strong signal cross-correlation while still being able to observe the desired weak signal [33]. These new codes are slightly modified versions of the original codes, which are more orthogonal to strong signals and aim to provide the original codes with some immunity to interferences, and they have the property of being able to extract the component of the weak signal subspace that does not lie within the strong interfering signal subspace. Nonetheless, they require a significant amount of matrix operations to construct the codes which could be a problem in real-time.

In both interference cancellation and subspace projection techniques, estimation of the parameters of the strong signals is needed for further signal reconstruction, but since they are the result of an estimation process, they inevitably contain errors. The former are found to be very sensitive to signal reconstruction errors, reducing their effectiveness. Moreover, the methods are further complicated by strong signal multipath and data-bit modulation, which can lead to a raise of the noise floor or even introduce additional interference [33]. The implementation of SIC/PIC also requires storage of a significant number of IF samples [28], which also translates into higher complexity in terms of storage memory, and continuous adjustment and monitoring of the satellite which is being subtracted needs to be done due to time and frequency variations. This last issue is a recognized difficulty in SIC. With this being said, the subspace projection technique was chosen to be analysed for near-far mitigation in the HISENS project.

<u>Subspace Projection Technique</u>

Since an estimation of the strong interfering signal is needed for the reconstruction of the strong signal, there are many factors that may affect the accuracy of such reconstruction, leading to situations in which a portion of the interference still remains in the projected signal. These factors can be estimation errors in the synchronization parameters (Doppler shift, code delay) of the strong signal, as well as the effects of filtering the input signal, quantization of the input signal or misdetection of data bits in the data channel.

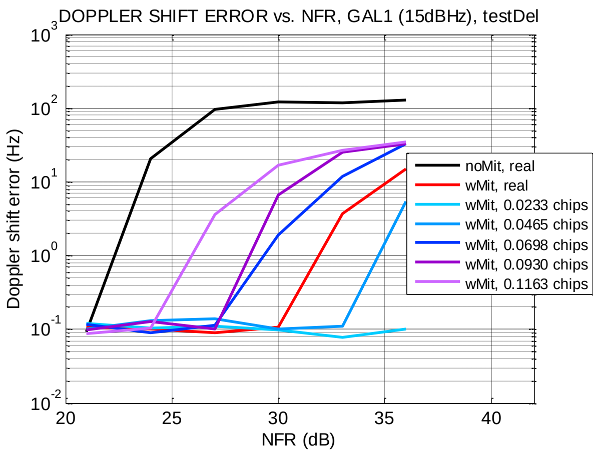

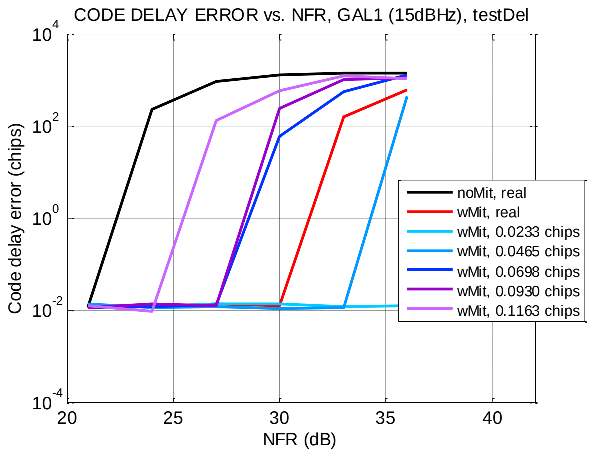

Figure 12 Mean absolute Doppler and code-delay estimation errors in the weak signals acquired after near-far mitigation for different code-delay estimation errors of the strong interfering signal, for different values of NFR. The case labelled as "real" corresponds to the situation where the errors in the parameters of the strong signal are simply those obtained in its acquisition

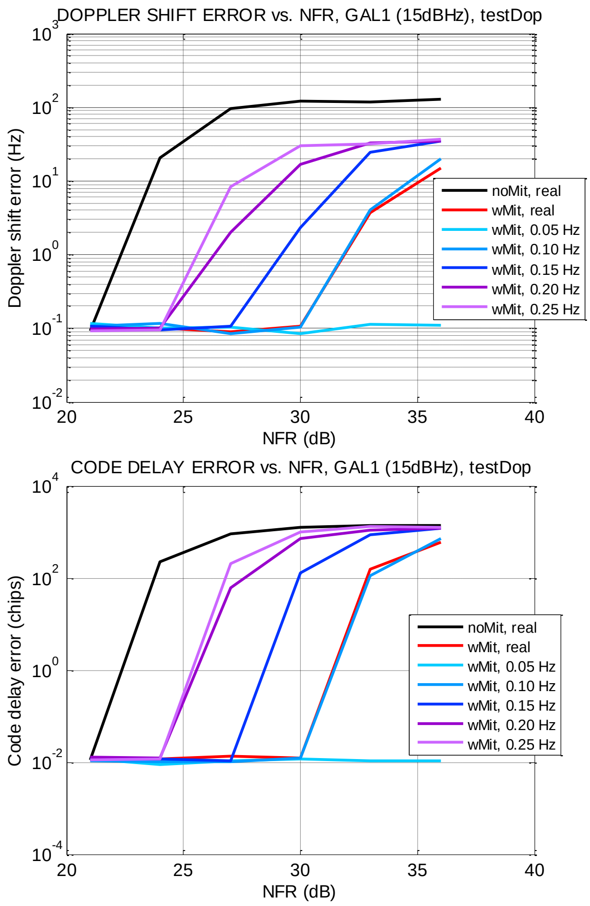

Figure 13 Synchronization errors present in weak signals acquired after near-far mitigation for different estimation errors of the Doppler shift of the strong interfering signal, affecting the reconstructed version

The following conclusions have been extracted:

- Even in the presence of code-delay and Doppler estimation errors in the parameters of the strong signal, the subspace-projection technique attenuates the strong signal in 15dB, which provides enough additional protection for practical cases of near-far interference. Frequency estimation errors have a more deleterious effect, as it could be expected since they produce cumulative errors between the real interfering signal and the reconstructed one, which becomes more and more evident as the correlation time increases.
- The filtering of the input signal to 4, 8 and 12 MHz reduces the mitigation of the strong signal in 6, 4 and 3dB, respectively, with respect to the non-bandlimited case. This implies that the subspace-projection technique can be applied even when the input signal is strongly filtered to 4MHz, and near-far ratios on the order of 30dB can be confronted, which means that the technique is robust enough to withstand virtually all practical conditions.
- The subspace-projection mitigation is hardly affected by the quantization of the input signal as long as the mitigation is done in high-accuracy (i.e. floating point) arithmetic. This is the usual approach in software-defined receivers. The mitigation works satisfactorily even when the signal is quantized with 2 bits, which is a usual case in commercial front-ends. In case the mitigation is done with finite arithmetic, then the result published in [34] is applicable.
- As far as bit errors are concerned, the subspace-projection technique is also able to sustain relative large values of the BER. For instance a BER=10% produces a degradation of around 2dB with respect to the near-far mitigation achieved in the absence of bit errors.

Multipath Detection

The literature about multipath detection is very limited compared to multipath mitigation. Some techniques revolve around identifying the different components that form the total correlation and try to isolate the contribution of the LOS. Another group of techniques exploits the fact that multipath is always delayed with respect to the LOS and this causes an asymmetric effect on the correlation curve. Among the former group, there are techniques exploiting the correlation peak asymmetry in presence of multipath. Two multipath detection methods were analysed:

- <u>Slope Asymmetry Metric</u> (SAM): is obtained by comparing the left and right slopes of the received signal correlation peak [35]. Ideally, both slopes should be equal and sign reversed, thus their sum should be theoretically close to zero.
- <u>Slope Coherence Time</u> (SCT): if the SAM is obtained for several snapshots, the time covariance of the SAM will be affected by the presence of multipath [35].

In the analysis it was observed that SAM and SCT are useful techniques to detect multipath that is coherent with the LOS signal. For high-sensitivity applications, which demand long coherent integration periods, coherent multipath is present mainly in static or low dynamic scenarios because the multipath components with a moderate Doppler spread are filtered out by the long coherent correlation process (multipath components with moderate Doppler spread become incoherent with the LOS signal when the integration time is longer than the inverse of the Doppler spread and hence they do not affect the LOS correlation curve), which is an advantage. Therefore, depending on the Doppler spread of the multipath, its effect may be visible on the mean or on the variance of the SAM, and in the latter case, the SCT may provide useful information about its value. Finally, the occurrence of NLOS produces an increase of the SAM variance

INNOVATIVE CLOSED-LOOP TECHNIQUES

Three types of closed loop techniques were reviewed:

- Optimisation of constant bandwidth tracking
- Adaptive bandwidth tracking
- KF-based tracking

The main reference for the first type of techniques is the DLL/ PLL classical receiver architecture. The most relevant technique among this family to be analysed is the DLL/ FPLL. In this configuration, the PLL is aided by a FLL, providing potentially more robustness and adaptability. Finally, DLL/ FLL architecture will also be analysed as reference, since it can be relevant for the transition from acquisition to tracking.

Regarding the last two families, the best performance is achieved with an adaptive-R Kalman Filter (AKF) since it provides a systematic approach for the dynamic definition of the bandwidth according to the environment – in this case driven by CN0. It is based on leaving the model uncertainty fixed, $\sigma^2_{Q,k} = \sigma^2_Q$, and then letting the measurement noise $\sigma^2_{R,k}$ evolve as a function of time. The advantage of this approach is that we can easily cope with weak signals by adjusting $\sigma^2_{R,k}$ accordingly, so as to match the current working conditions [36], [37], [38].

As a conclusion, the following techniques were analysed: DLL/FLL, DLL/PLL, DLL/FPLL and AKF/PLL. The analysis covered simulations with AWGN, static and dynamic multipath and space applications using ESA's ADAPT platform [39], a semi-analytical platform (not bit-true) that allows comparing the tracking loop techniques testing them in a wide variety of conditions.

AWGN Sensitivity

An **indoor static** environment was tested with the semi-analytical platform to see the best performances the techniques can achieve when the signal had no dynamics at all. The obtained results showed that all the techniques can track code down to a CN0 of 0dB-Hz (this low C/N0 is possible because the semi-analytical platform simulated a completely static test without satellite dynamics), but when it comes to robustness the DLL technique presents better results than the AKF, with an inferior number of loss-of-lock iterations. It has been observed that in order to use the adaptive mechanism of the AKF a good CN0 estimator capable of working at low CN0 environments is required (which is very difficult). Fixing the CN0 input with a low value, presents similar performance to the DLL, so this AKF (with fixed low CN0) can also be seen as a candidate. Regarding phase tracking, the PLL can track down to 0 dB-Hz, but the FPLL only is capable of tracking down to 10 dB-Hz (the FLL component is does not bring any advantage for static scenarios), having less robustness than the PLL. For these reasons the most reliable technique is the PLL/DLL. When it comes to modulations the GPS L5 presents the best accuracy due to its chip size and the GPS L1 C/A is very similar to the Galileo E1C.

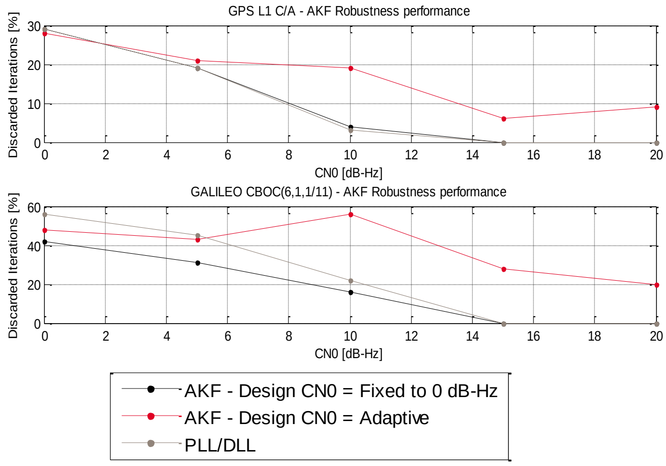

Figure 14 Robustness performance of the AKF for GPS and GALILEO - Static

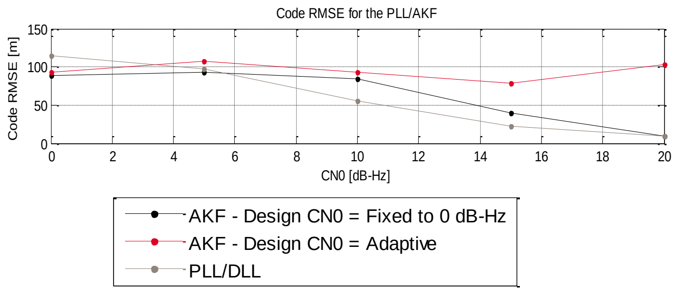

Figure 15 AKF code RMSE for CBOC(6,1,1/11) - Static

For the **indoor pedestrian dynamics** scenario the tracking limits are higher than in the static one. Code tracking is only possible for CN0's higher than 10 dB-Hz; there is the need to increase the integration time to "reject" the noise but with dynamics this time cannot be very high and because of that it is not possible to track for very low CN0's. Phase tracking is only possible for CN0's higher than 15dB-Hz.

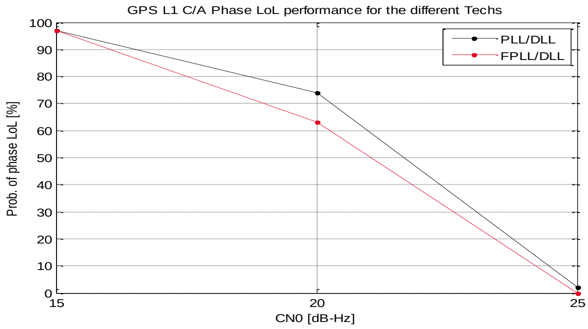

Figure 16 Prob. of phase LoL for GPS L1 C/A - Dynamic

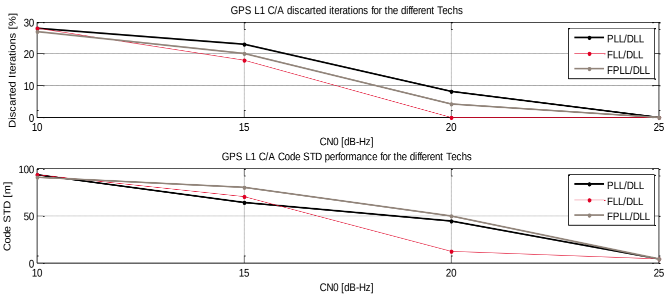

Figure 17 Code tracking performance for GPS L1 C/A - Dynamic

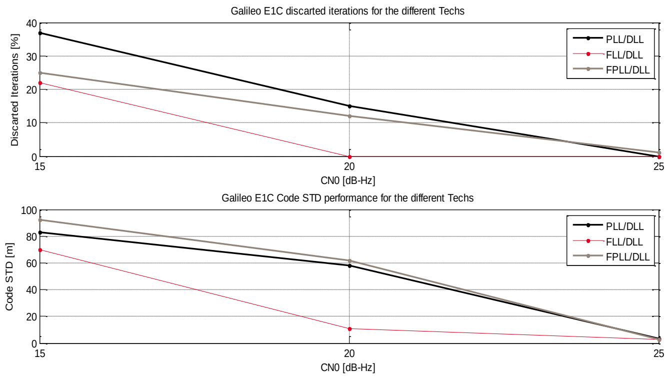

Figure 18 Code tracking performance for Galileo E1C - Dynamic

When it comes to the techniques, the most robust and accurate code tracking technique configuration is the DLL/FLL, due to the fact that it can handle higher integration times than the PLL and FPLL and it is better in following the user dynamics, providing better results when acceleration is present. Unfortunately the FLL cannot track phase, but frequency, therefore if there is the need to track phase the FLL cannot be considered and FPLL is then preferred.

Static and Dynamic Multipath

In the **static multipath** scenario we have seen that code tracking can be maintained below 15dB-Hz for GPS L1 C/A while Galileo E1 CBOC(6,1,1/11) appears to struggle in low CN0 environments, only presenting reasonable results above 15 dB-Hz. The CBOC modulation appears to only present an advantage over the GPS L1 BPSK(1) for CN0 values above 20dB-Hz. Note that at this CN0 level the CBOC ACF shape becomes an advantage, due to its sharper and narrower main peak, allowing a better code tracking resolution.

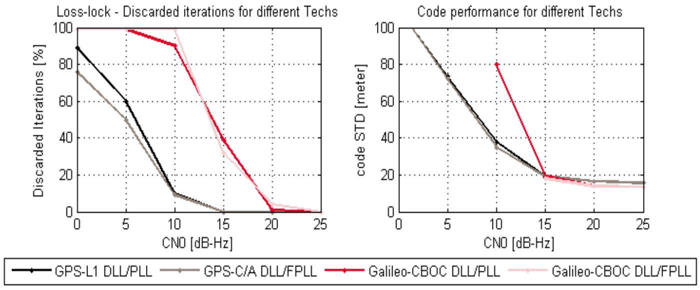

Figure 19 Multipath: comparison of results - Static

In the case of **dynamic multipath** we have seen that the carrier-techniques have a lot of problems when dealing simultaneously with user dynamics and low CN0 environments. From all the techniques used, FPLL presents better phase and Doppler estimates between 15dB-Hz and 25dB-Hz and should be considered in scenarios where dynamics are involved. Nevertheless phase tracking is very difficult below CN0 of 15dB-Hz and should not be expected.

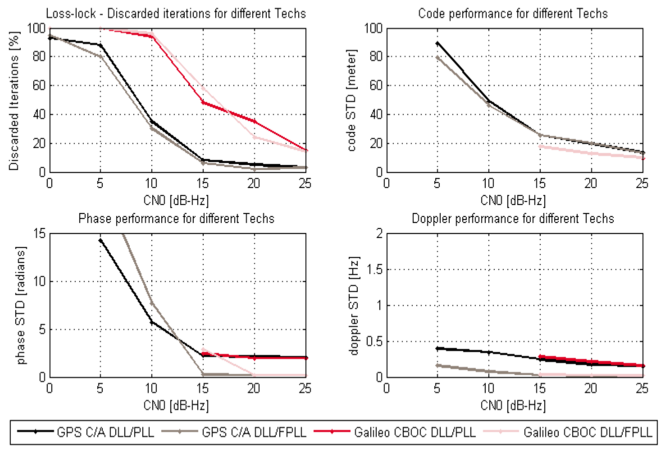

Figure 20 Multipath: comparison of results - Dynamic

Space Applications

The scenarios involving satellite orbits have shown to be very challenging. The first test case considered the possibility to have data demodulation during an **orbital manoeuvre** for LEO and GEO. We have seen that for LEO using a data channel code and phase tracking is not possible for CN0 values below 30dB-Hz. It appears that the carrier techniques were not able to handle simultaneously the tasks of dynamic tracking, noise rejection and data demodulation. For a GEO orbital manoeuvre it is possible to have GPS L1 C/A data demodulation for CN0 values down to 22.5dB-Hz with 50% of data demodulation probability and 25dB for 90%.

When testing **sensitivity to dynamics** for orbital manoeuvres, it was seen that seen that the higher the initial Doppler error the higher the probability of the iterations to be in loss-of-lock. Recall that this initial error was introduced in order to simulate the acquisition process. Furthermore it was identified that below CN0 of 20dB-Hz it becomes very difficult to correct these errors.

Regarding the techniques, the performance of the configurations DLL/FPLL and DLL/PLL is very similar in terms of code robustness, but when it comes to phase robustness the FPLL presents better results than the PLL (the PLL loses lock and the FPLL has cycle slips, which do not threaten the data demodulation) for data demodulation purposes.

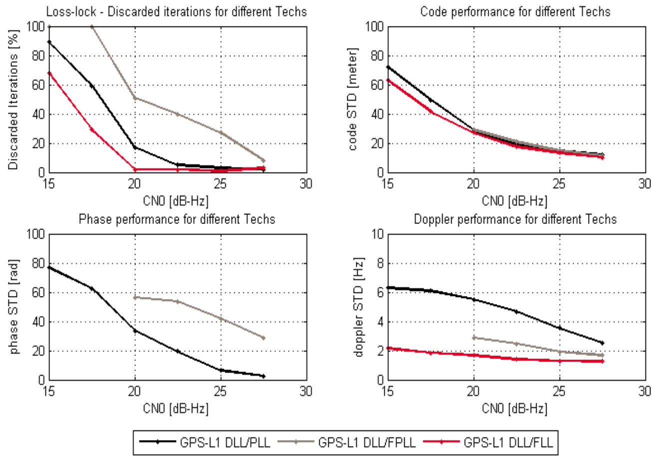

Figure 21 GPS L1 C/A comparison of results – High Dynamics

Manoeuvre-like environment was also tested for a LEO satellite without data demodulation. We have seen that it is possible to have code and phase tracking during manoeuvres for CN0 around 25dB-Hz. Below this threshold it becomes very difficult for the carrier techniques to deal both with dynamic stress and noise rejection.

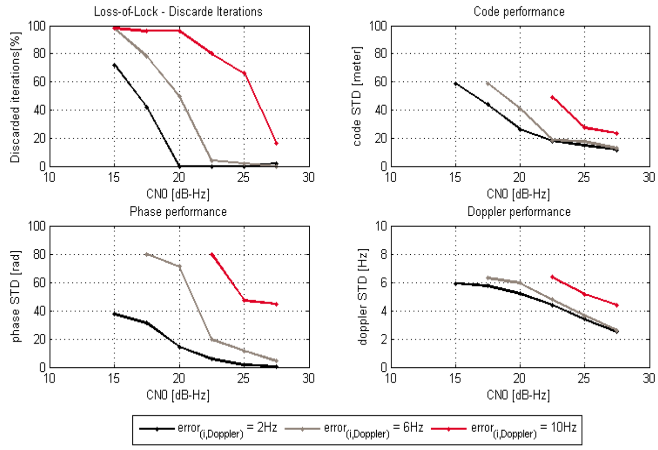

Figure 22 Analysis of tracking performance for different initial Doppler errors – High Dynamics

Overall, the technique that performed the best for carrier tracking was FPLL, since it could deal with higher order dynamics better than PLL and it could provide phase tracking, something that FLL cannot do.

Remarks

For code tracking the best performances are provided by the conventional DLL and AKF but fixing the estimated C/N0 at low levels. Regarding phase there are some good candidates depending on the scenario. For static users the conventional PLL should be used. Nevertheless if dynamics are involved then it might be best to use FPLL. Also, adaptive-bandwidth PLL (APLL), which incorporates a loop bandwidth adaptive mechanism based on the C/N0 level, was considered as a candidate technique.

It was seen that carrier tracking below 15dB-Hz is in general very difficult if not impossible. Therefore at this level, carrier techniques that minimize the noise should be used: PLL, and in the case of dynamics, FLL. For CN0 above 15dB-Hz it as seen that FPLL performed the best for dynamics and PLL for static.

Furthermore and based on this information a new architecture should be considered, one that allows carrier tracking to switch between techniques, PLL to FPLL or FLL before declaring loss-of-lock, since it is possible to have code tracking without phase tracking. Such architecture could minimize the declaration of losses-of-lock and avoid the acquisition process which can be very time and resource consuming.

SELECTED HIGH-SENSITIVITY TECHNIQUES

The following high-sensitivity GNSS signal processing techniques were selected to be tested with the HISENS PoC Demonstrator at GPS L1 and L5 and Galileo E1 and E5a bands. The list includes some novel techniques, in particular for non-coherent integration and near-far detection:

- Open-loop / Snapshot Techniques (Acquisition):
  - Advanced correlation techniques
    - Non-coherent Post-Detection Integration (NPDI) [as baseline]
    - Generalized Truncated Post-Detection Integration plus Squaring Detector (GPDITSD)
    - Generalized Truncated Post-Detection Integration (GPDIT)
  - NF Detection Techniques
    - Probability of threshold crossing
    - Chi-square Goodness of Fit (GoF)
  - NF Mitigation Technique
    - Subspace projection technique
  - Multipath Detection
    - Slope Asymmetry Metric (SAM) (mean, variance and SCT)

- Closed-loop Techniques (Tracking):
  - DLL for code, PLL for phase [as baseline]
  - DLL for code, FLL for frequency
  - DLL for code, FPLL for phase
  - DLL for code, APLL for phase
  - Adaptive Kalman Filter (AKF) for code, PLL for phase

HISENS PoC DEMONSTRATOR

After reviewing the different high sensitivity techniques a Proof of Concept demonstrator was developed in order to test the selected techniques with RF signals obtained from a simulator and from real field tests.

The Proof of Concept (PoC) demonstrator is a hardware and software platform capable of collecting RF samples and testing different GNSS high sensitivity techniques (snapshot and closed-loop). It is based on quasi-open loop and closed loop architectures.

The following figures show the high level design of the whole platform and its physical architecture:

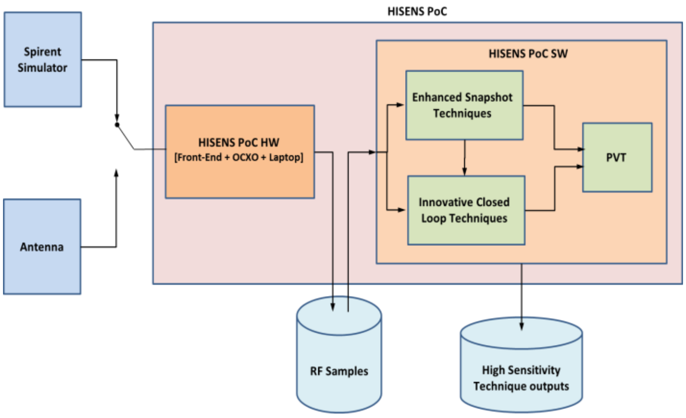

Figure 23 High level design of the PoC

The PoC HW platform is formed by the following elements:

- GNSS Antennas: two different antennas are used, one dual-band high-grade antenna (Novatel GPS-703-GGG) and a low quality patch antenna (Taoglas L1 patch antenna).
- Amplifier+Splitter: used to feed the RF signal to the two channels in the Front-End to take samples in L1 and L5 bands at the same time (GPS Source 2-Way Splitter).
- GNSS RF Front-End: the Tecnalia HORUS3000 multi-constellation GNSS RF-FE is a superheterodyne RF Front-End with 4 channels, each with an independent LO (programmable PLL) to receive any GNSS frequency bands from 1 to 2GHz. HORUS3000 connects to a Xilinx FPGA evaluation board by means of a LPC FMC connector.
- OCXO: A medium-grade OCXO, very stable in the short term (to allow long integration times) is employed to feed the Front-End (Axtal AXIOM95).
- Laptop: Connected to the Xilinx FPGA is used to store the RF samples collected by the Front-End.

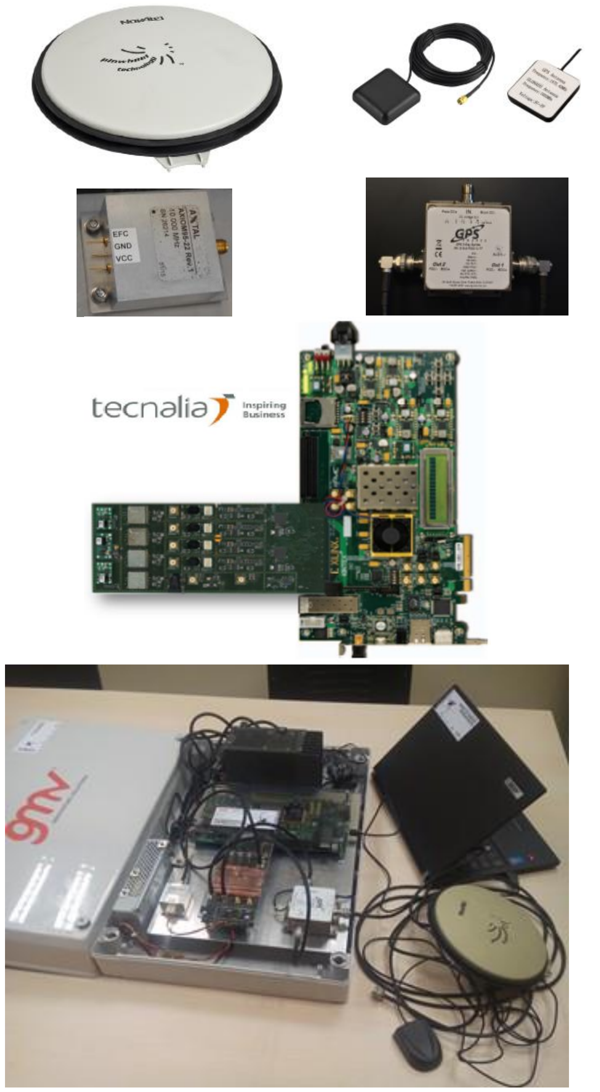

Figure 24 HISENS PoC HW elements

The PoC SW platform is a high-sensitivity SW receiver formed by the following elements:

- Open-Loop module: implements the selected enhanced snapshot high-sensitivity techniques capable of acquiring the GPS (L1 C/A and L5-Q) and Galileo (E1C and E5a-Q) signals stored in the RF sample files collected by the Front-End. It is based on an evolution of ESA's DINGPOS platform [40].
- Closed-Loop module: implements the selected closed-loop techniques capable of tracking the GPS (L1 C/A and L5-Q) and Galileo (E1C and E5a-Q) signals stored in the RF sample files collected by the Front-End. The tracking is started using the code delay and Doppler estimated by the open-loop techniques. It is based on an evolution of ESA's ROCAT bit-true platform.
- PVT module: it provides a PVT solution (weighted LS with meas. rejection) using the code delays and the Doppler measurements estimated by the acquisition or the tracking modules. The code ambiguity is solved by using the technique described in [41].

TEST CAMPAIGN

The HISENS test campaign covered the following use cases:

- Static Indoor (SI)
- Dynamic Indoor (DI)
- Urban Canyon (UC)
- Space Applications (SA)

Four signals were selected to be processed in the tests, being most of them pilot signals to allow increasing the coherent integration time:

- GPS L1 C/A: BPSK(1)
- GPS L5-Q: BPSK(10)
- Galileo E1C: CBOC(6,1,1/11)
- Galileo E5a-Q: AltBOC(15,10)

There were two different types of test cases with respect to the way in which the RF samples were collected:

- Simulation: the GNSS RF signal was generated using ESA's GSS9000 Spirent simulator at ESTEC's GNSS Lab. The four use cases were tested with the simulator setting accuracy, robustness and sensitivity tests (decreasing the C/N0 of the signals in steps of several seconds) for indoor and urban use cases, and different parts of LEO, HEO and GEO orbits for space applications.
  As the Spirent simulator allows complete control of the generated signals, a complete L1&L5 GPS constellation was simulated along with a fully populated Galileo constellation. Also, to increase the coherent integration time the pilot signals were used, and in the case of the GPS L1 C/A the navigation message bits were forced to a constant state (i.e. setting all bits to 0), thus simulating as if the navigation data would have been wiped-off.
  The multipath environment was simulated configuring the Land Mobile Multipath (LMM) model in the Spirent simulator for indoor ([42]) and urban ([43] [44]) tests. Also two urban canyon tests were configured using the DLR model ([45] [46]).

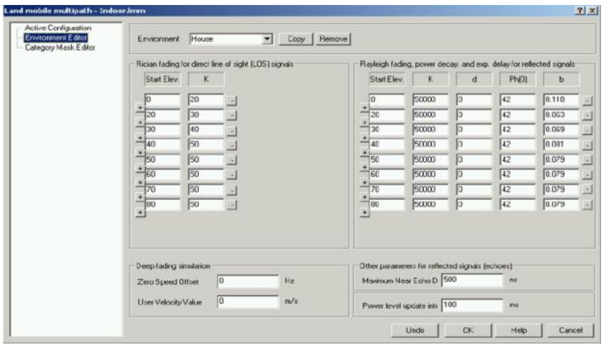

Figure 25 Indoor Rician and Rayleigh fading configuration parameters

Type	Elevation (deg)	K
Urban	0-20	5
	20-40	18
	40-65	46
	65-90	62

Type	Echo Number	Delay Max (ns)
Urban	1	600

Type	Elev (deg)	K Rayleigh	d	Ph(0)	b Delay
			Mean Loss		
Urban	0-15	15	11	-16	0.118
	15-30	20	25	-18	0.066
	30-55	25	7.5	-23	0.075
	55-90	50	6	-26	0.080

Table 2 Urban Canyon Rician and Rayleigh fading configuration parameters

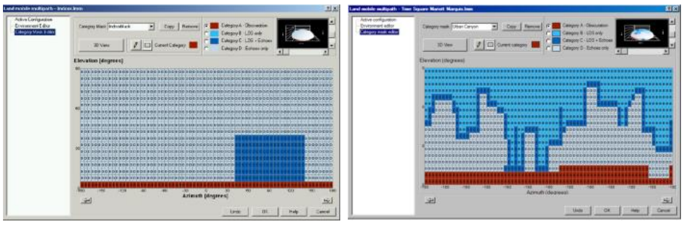

Figure 26 Indoor and Urban Canyon LMM elevation-azimuth Masks

- Field: the field test cases were recorded on real environments like GMV office or in urban canyons in the city of Madrid. All the use cases except for the space applications were also tested with field data. As mentioned, pilot signals were used to avoid the navigation message bit transitions in long coherent integration times, and in the case of GPS L1 C/A a coherent integration time of 20 ms was used increasing the number of non-coherent integrations instead.

Figure 27 Indoor Field Tests at GMV

Figure 28 Urban Field Tests in Madrid

TEST RESULTS

Some of the most relevant results obtained when processing the data collected during the test campaign are presented in this section.

Sensitivity Tests

In the sensitivity tests the C/N0 was configured to decrease with time. Thus, the following figures show how lower C/N0 can be acquired when the integration time is increased.

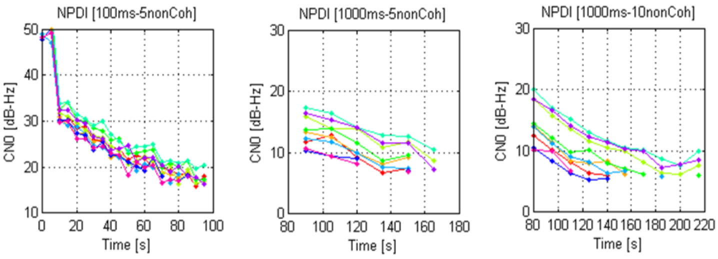

Figure 29 Static Indoor Sensitivity Test Results – NPDI GPS L1 C/A (data wiped-off)

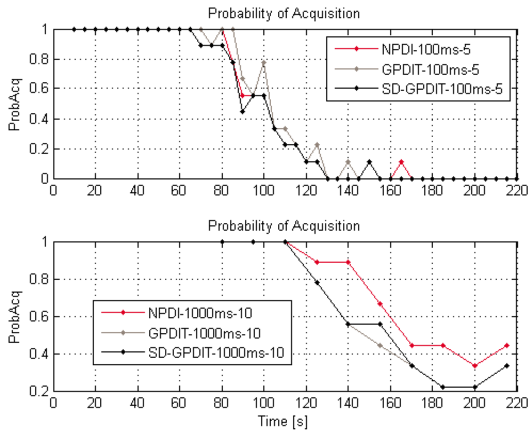

Figure 30 Static Indoor Sensitivity – Comparison of probability of acquisition for different techniques: GPS L1 C/A (data wiped-off)

With an acquisition integration length of 500ms it is possible to have good acquisition results at C/N0 values down to 20dB-Hz. Below this empirical threshold acquisition length must be increased to values up to 5 s. With this configuration it is possible to acquire signals around or below 10dB-Hz, and also with an integration length of 10 s signals with a C/N0 close to 5dB-Hz. But with 10 s the results were not considerable better than with 5 s in order to justify using such a long acquisition length. It is important to remark that as the acquisition integration time increases so does the memory and time required to process the simulation. Similar results were obtained for GAL E1C.

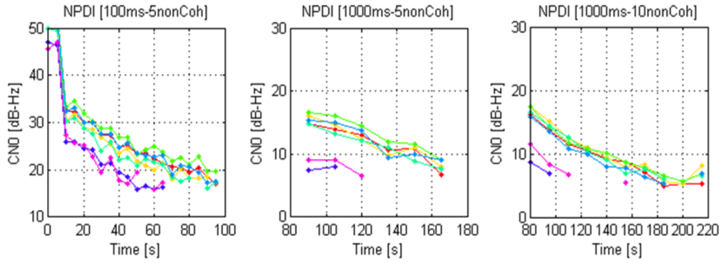

Figure 31 Static Indoor Sensitivity Test Results – NPDI GAL E1C

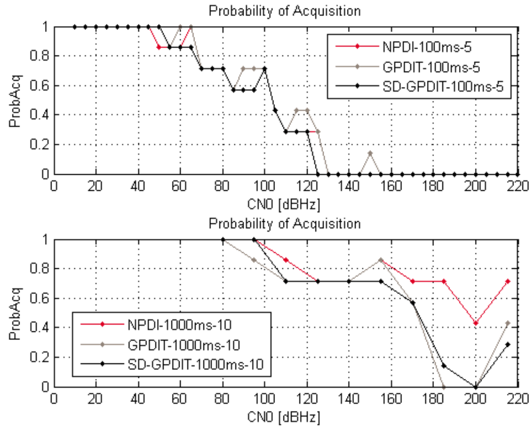

Figure 32 Static Indoor Sensitivity – Comparison of probability of acquisition for different techniques: GAL E1C

In both GPS L1 C/A and GAL E1C results it can be seen that NPDI method shows better probability of acquisition than the GPDIT and GPDITSD for long integration time values. However, the GPDIT may provide an improvement over the NPDI method as, theoretically, the larger the number of non-coherent correlation, the more difference might exist between the GPDIT and the NPDI in a Gaussian channel. This issue is currently under analysis.

Similar results are obtained in the dynamic indoor and In the urban canyon sensitivity tests:

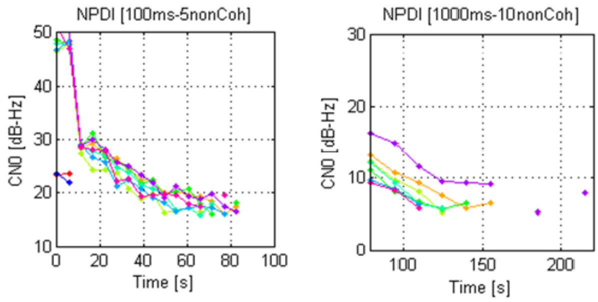

Figure 33 Dynamic Indoor Sensitivity Test Results – NPDI GPS L1 C/A (data wiped-off)

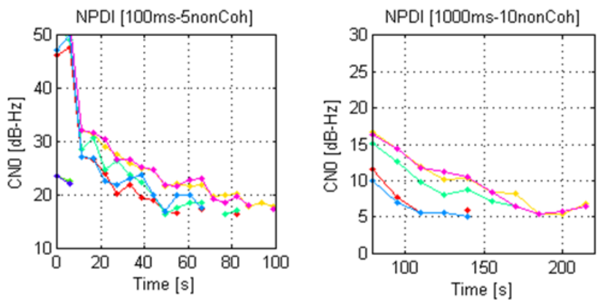

Figure 34 Dynamic Indoor Sensitivity Test Results – NPDI GAL E1C

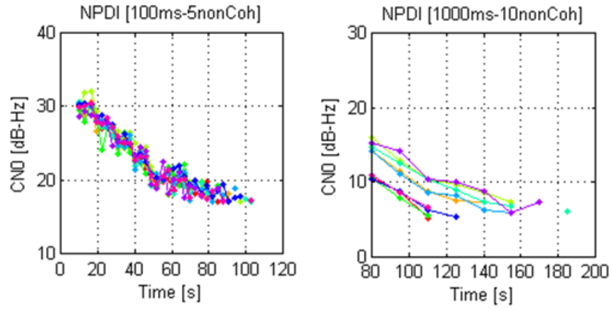

Figure 35 Urban Canyon Sensitivity Test Results – NPDI GPS L1 C/A (data wiped-off)

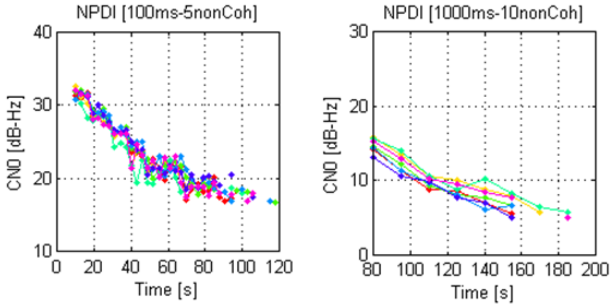

Figure 36 Urban Canyon Sensitivity Test Results – NPDI GAL E1C

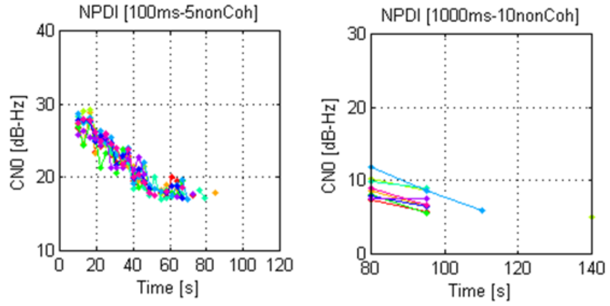

Figure 37 Urban Canyon Sensitivity Test Results – NPDI GPS L5-Q

SAM

In Figure 38 it is possible to see the SAM results evaluating the distortion of the correlation peak (mainly due to multipath effects). Note that the distortion effect on SV27 can be clearly identified with this metric. When multipath is present and affects the correlation peak SAM provides high positive or negative values.

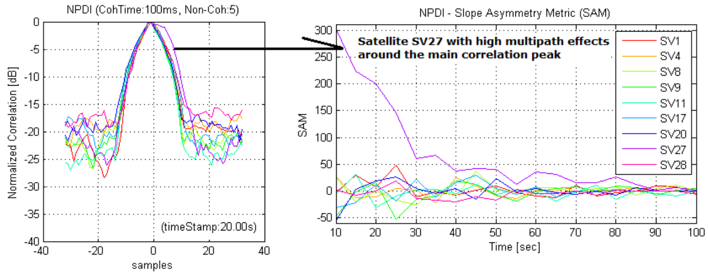

Figure 38 Static Indoor Sensitivity Test: SAM Results – GPS L1 C/A (data wiped-off)

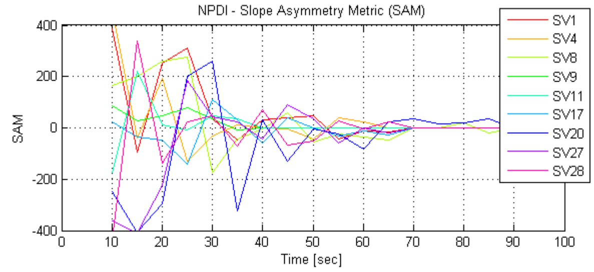

Figure 39 Static Indoor Sensitivity Test: SAM Results – GPS L5-Q

The SAM metric has also proved to be a good indicator of the presence of multipath in the simulated accuracy and in the real field tests:

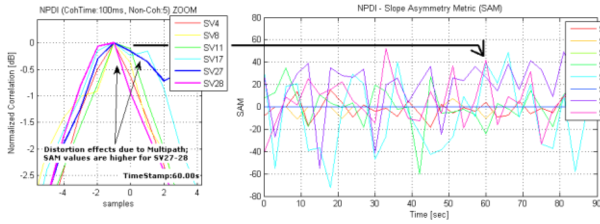

Figure 40 Static Indoor Accuracy Test: SAM Results – GPS L1 C/A (data wiped-off)

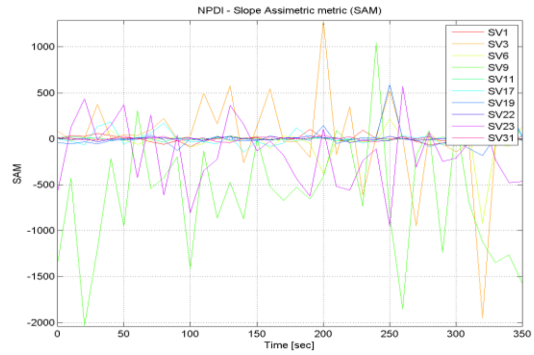

Figure 41 Urban Canyon Field Test: SAM Results – GPS L1 C/A (CohTime: 20ms, Non-Coh: 25)

Near-Far Mitigation

The next figures present a test for NPDI with and without Near-far mitigation. It is possible to see that when the mitigation is used the NPDI technique is able to identify a satellite previously not acquired.

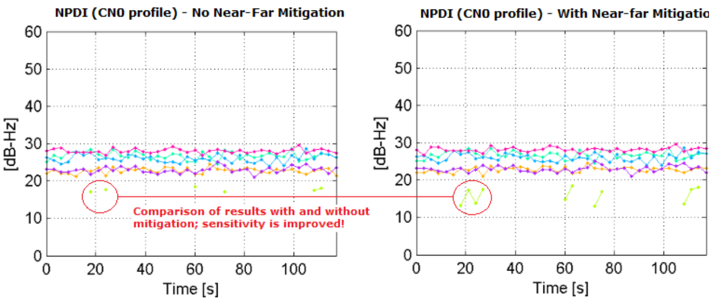

Figure 42 Static Indoor: Comparison of results with and without Near-Far Mitigation for L1CA with NPDI

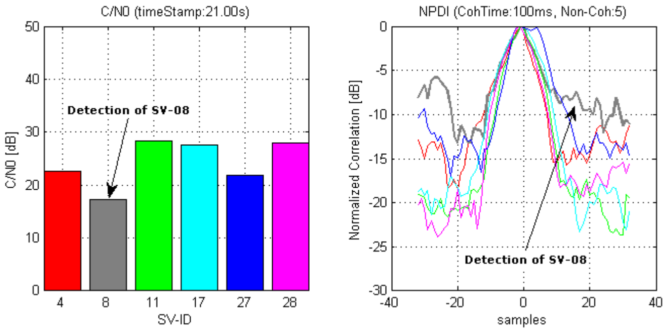

Figure 43 Static Indoor: Snapshot for NPDI with Near-Far Mitigation (L1CA)

Closed-Loops

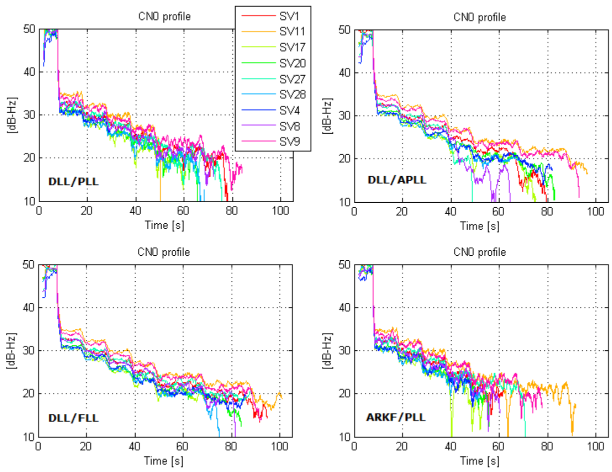

Figure 44 Static Indoor Sensitivity Test: Closed-Loop Results – GPS L1 C/A (data wiped-off)

Figure 44 presents the results obtained in the static indoor sensitivity test with the different closed-loop techniques configurations. The best sensitivity results are obtained with DLL(40ms)/FLL(40ms) followed by DLL(40ms)/APLL(10ms). With both configurations it is possible to have tracking for most satellites in a period where CN0 is just below 20dB-Hz.

Figure 45 and Figure 46 provide the temporal STDEV (using a sliding window) of the code delay and Doppler measurements . Note that the code STDEV results with AKF appear more stable than DLL, despite the longer integration time of 40ms. This is a result of using a Kalman-type filter which provides the best configurations at each time instant. Also note that the FLL presents better results (more stable and lower amplitude) than PLL. This result is a translates of the fact that PLL tracks phase and only afterwards derives Doppler-frequency estimates while the FLL directly tracks Doppler-Frequency but does not provide any information about phase measurements.

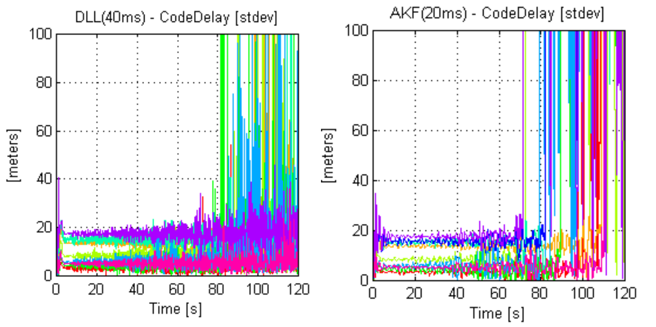

Figure 45 Static Indoor Sensitivity Test: Closed-Loop Code STDEV – GPS L1 C/A (data wiped-off)

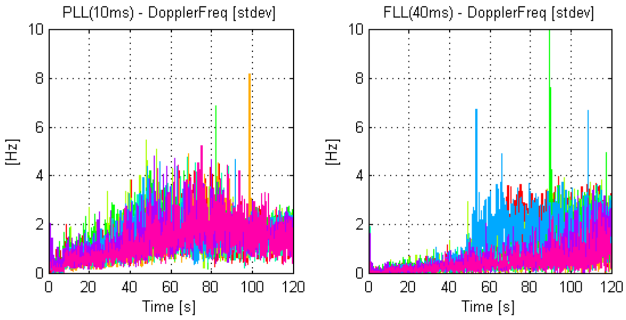

Figure 46 Static Indoor Sensitivity Test: Closed-Loop Doppler STDEV – GPS L1 C/A (data wiped-off)

Figure 47 presents the results obtained in the urban canyon sensitivity test with the different closed-loop techniques configurations. The best sensitivity results are obtained with DLL(40ms)/FLL(40ms) followed by DLL(40ms)/APLL(10ms). With both configurations it is possible to have tracking for most satellites in a period where CN0 is just below 20dB-Hz.

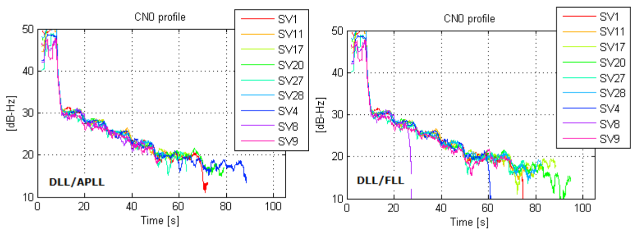

Figure 47 Urban Canyon Sensitivity Test: Closed-Loop Results – GPS L1 C/A (data wiped-off)

Accuracy

The code delays and Doppler measurements allow to provide a valid PVT solution. The PVT algorithm in the PoC SW platform is a weighted Least-Squares with measurement rejection that also has to estimate the coarse time. It needs an initial PVT state close to the actual one to start the first iteration. It should be taken into account that each computed PVT solution is independent from the others (no filtering is performed). The following figures show some examples of the PVT solution obtained in the tests:

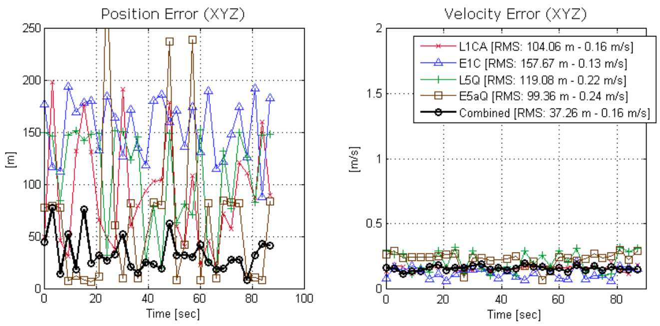

Figure 48 Static Indoor Accuracy Test: PV Results – NPDI 500ms

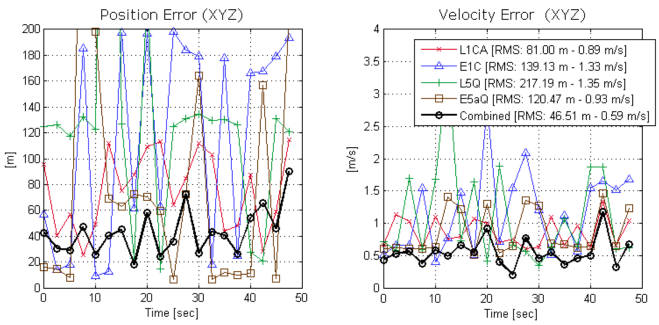

Figure 49 Dynamic Indoor Accuracy Test: PV Results – NPDI 500ms

Figure 50 Urban Canyon Field Test: PV Results – NPDI 1000ms

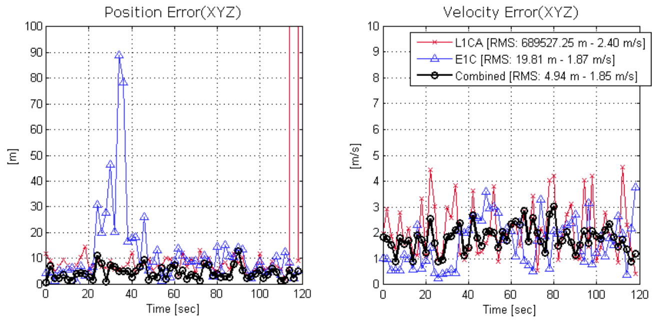

Figure 51 Space Applications LEO Pole Test: PV Results – NPDI 500ms

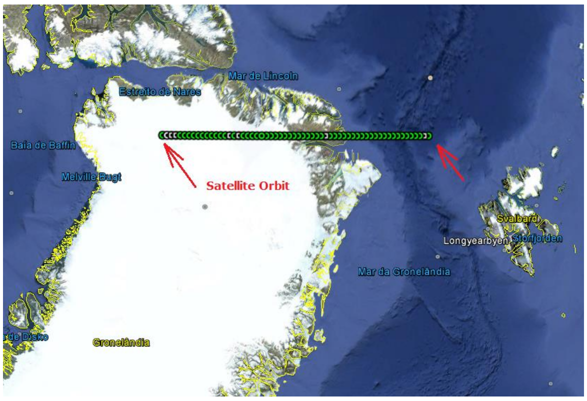

Figure 52 Space Applications LEO Pole Test: Orbit trajectory on Google-Earth – 500ms

With respect to the coarse time estimation, the typical deviation of the combined solution is around 15-30 ms in indoor and urban tests and around 1 ms or less in space application tests.

CONCLUSIONS

A complete overview of the leading edge high-sensitivity techniques has been provided in the first part of the paper along with the analysis of their performances based on simulations. Thus, contributing to understand the high-sensitivity challenges and to identify the most promising techniques.

The PoC demonstrator has been described along with the different tests aiming to cover the four use cases relevant for the application of high sensitivity techniques:

- Static Indoor (SI)
- Dynamic Indoor (DI)
- Urban Canyon (UC)
- Space Applications (SA)

The test results have been obtained using real signals and signals generated with a Spirent simulator (GSS9000) and collected with a dual-frequency Front-End. The different techniques were tested with GPS L1 C/A and L5-Q and Galileo E1C and E5a-Q signals.

A wide variety of techniques have been tested with the RF samples collected with the Spirent simulator and in the real field tests, allowing to assess the performances of the leading-edge acquisition/open-loop advanced correlation techniques (e.g. GPDITSD and GPDIT) and tracking/closed-loop high sensitivity techniques (e.g. AKF). For example, the obtained results have demonstrated that with long integration times enhanced snapshot techniques can acquire signals below 10 dB-Hz. Besides, assessing the performance of the high sensitivity techniques will also aid any potential application to clarify what can be achieved with these techniques.

Finally, the data already collected in the tests and the described PoC demonstrator, which was especially designed for collecting RF samples and testing the high sensitivity techniques with them, represent a powerful tool for future improvements or research in any of these techniques.

REFERENCES

[1] D. Jiménez-Baños et al., “Innovative techniques for GPS indoor positioning using snapshot receiver”, Proc. Institute of Navigation (ION), 2006.

[2] G. Seco-Granados et al., “Challenges in Indoor Global Navigation Satellite Systems: Unveiling its core features in signal processing”, Signal Processing Magazine, IEEE (Volume:29 , Issue: 2), March 2012.

[3] O. Julien, G. Lachapelle and M. E. Cannon, “Galileo L1 Civil Receiver Tracking Loops’ Architecture”, IEEE International Symposium on Circuits and Systems, 2007. ISCAS 2007.

[4] O. Julien, “Design of Galileo L1F Receiver Tracking Loops”, University of Calgary PhD Thesis, July 2005.

[5] N. Sokhandan, “A Novel Multipath Estimation and Tracking Algorithm for Urban GNSS Navigation Applications”, ION GNSS+ 2013, September 2013.

[6] Z. He and M. Petovello, “Multipath Mitigation by Voting Channel Impulse Response in Navigation Domain with High-sensitivity GNSS Receivers”, ION GNSS+ 2013, September 2013.

[7] A. Fernández et al., “Innovation: Hunting for GNSS Echoes - Analysis of Signal Tracking Techniques for Multipath Mitigation”, GPS World, November 2, 2013.

[8] C. Gentner, T. Jost and A. Dammann, “Accurate Indoor Positioning using Multipath Components”, ION GNSS+ 2013, September 2013.

[9] S.H. Kong, W. Nam, “A-GNSS sensitivity for parallel acquisition in asynchronous cellular networks” Wireless Communications, IEEE Transactions on, 9(12), 3770-3778.

[10] B. Soltanian, A.M Demirtas, and M. Renfors, “Reduced-complexity FFT-based method for Doppler estimation in GNSS receivers”. EURASIP Journal on Advances in Signal Processing, 2014(1), 1-15.

[11] G. Seco-Granados, J. A. Lopez-Salcedo, D. Jiménez-Baños, G. López- Risueño, "Signal Processing Challenges in Indoor GNSS", IEEE Signal Processing Magazine, vol. 29, no. 2, pp. 108-131.

[12] D. Jiménez-Baños, G. López-Risueño, G. Seco-Granados, and A. García, “Innovative techniques for GPS indoor positioning using snapshot receiver,” in Proc. Institute of Navigation (ION), 2006, pp. 2944–2955.

[13] D. Jiménez-Baños, ““Enhanced Techniques for Indoor Positioning GPS Receivers”, ESA Report.

[14] N. Blanco-Delgado, D. Jiménez-Baños, G. Lopez-Risueño, G. Seco-Granados, "Efficient Algorithm for Galileo L1C Signal Acquisition in Weak Signal Environments", Proc. CNES Workshop on Galileo Signals and Signal Processing, Toulouse (France), Oct 2006.

[15] G. Lopez Risueno, G. Seco-Granados, "Method of Processing Positioning Signals, in Particular for Indoor Applications", patent number EP1994423B1, US2010/0061427, PCT/EP2006/002581, WO/2007/098787.

[16] A. Schmid, A. Neubauer. "Differential correlation for Galileo/GPS receivers." Acoustics, Speech, and Signal Processing, 2005. Proceedings.(ICASSP'05). IEEE International Conference on. Vol. 3. IEEE, 2005.

[17] H. Elders-Boll, U. Dettmar. "Efficient differentially coherent code/Doppler acquisition of weak GPS signals." Spread Spectrum Techniques and Applications, 2004 IEEE Eighth International Symposium on. IEEE, 2004.

[18] G.E. Corazza, R. Pedone. "Generalized and average post detection integration methods for code acquisition." Spread Spectrum Techniques and Applications, 2004 IEEE Eighth International Symposium on. IEEE, 2004.

[19] E. Lohan, J. A. Lopez-Salcedo, G. Seco-Granados, "Analysis of generalized post-detection integration techniques for the acquisition with pilot signals in high-sensitivity Galileo receivers", Proc. ESA Colloquium on Scientific and Fundamental Aspects of Galileo, Dec 05 2013

[20] S. Satyanarayana, D. Borio, and G. Lachapelle. "A non-coherent block processing architecture for standalone GNSS weak signal tracking." Proc. ION/GNSS, Portland, OR (2011): 1777-1785.

[21] T. S. Rappaport, "Wireless Communications. Principles and practice", Second Edition, 2002.

[22] E. D. Kaplan and C. Hegarty, “Understanding GPS Principles and Applications”, Second Edition. Artech House Publishers, 2006.

[23] B. Albright, "Essentials of Mathematicals Statistics", Jones & Burtlett Learning, Burlington MA, 1977.

[24] G. Lopez-Risueno, G. Seco-Granados, "CN0 estimation and near-far mitigation for GNSS indoor receivers," Vehicular Technology Conference, 2005. VTC 2005-Spring. 2005 IEEE 61st , vol.4, no., pp.2624,2628 Vol. 4, 30 May-1 June 2005.

[25] P.H Madhani, P. Axelrad, K. Krumvieda, J. Thomas, "Application of successive interference cancellation to the GPS pseudolite near-far problem," Aerospace and Electronic Systems, IEEE Transactions on , vol.39, no.2, pp.481,488, April 2003

[26] S. Verdu, "Multiuser detection", Cambridge University Press, United Kingdom, 1998

[27] B. Lu, J. Zhong, M. Zhao, L. Li , "A near-far effect canceller for GPS high sensitivity receiver," Position Location and Navigation Symposium (PLANS), 2012 IEEE/ION , vol., no., pp.341,346, 23-26 April 2012

[28] E. P. Glennon and A. G. Dempster, "A Review of GPS Cross Correlation Mitigation Techniques," presented at The 2004 International Symposium on GNSS/GPS, Sydney, Australia, 2004.

[29] L.Chen, W. Meng, S.Han, E.Liu, "A Cross-Correlation Mitigation Method Based on Subspace Projection for GPS Receiver," Proceedings of the 25th International Technical Meeting of The Satellite Division of the Institute of Navigation (ION GNSS 2012), Nashville, TN, September 2012, pp. 1428-1434.

[30] E. P. Glennon, R. C. Bryant , A. G Dempster, P. J. Mumford., "Post Correlation CWI and Cross Correlation Mitigation Using Delayed PIC,"Proceedings of the 20th International Technical Meeting of the Satellite Division of The Institute of Navigation (ION GNSS 2007), Fort Worth, TX, September 2007, pp. 236-245.

[31] Y. T. J. Morton, J.B.Y. Tsui, D. M. Lin, L. L Liou, M. M. Miller, Q. Zhou, M. P. French, J.Schamus, "Assessment and Handling of CA Code Self-Interference During Weak GPS Signal Acquisition," Proceedings of the 16th International Technical Meeting of the Satellite Division of The Institute of Navigation (ION GPS/GNSS 2003), Portland, OR, September 2003, pp. 646-653.

[32] F. D. Nunes, F. M. G. Sousa, "GNSS Near-Far Mitigation through Subspace Projection without Phase Information," Aerospace and Electronic Systems, IEEE Transactions on , vol.48, no.3, pp.2746,2755, JULY 2012

[33] É.P. Glennon, A.G. Dempster, "A Novel GPS Cross Correlation Mitigation Technique," Proceedings of the 18th International Technical Meeting of the Satellite Division of The Institute of Navigation (ION GNSS 2005), Long Beach, CA, September 2005, pp. 190-199.

[34] L. Chen, W. Meng, S. Han, E. Liu, "A Cross-Correlation Mitigation Method Based on Subspace Projection for GPS Receiver," Proceedings of the 25th International Technical Meeting of The Satellite Division of the Institute of Navigation (ION GNSS 2012), Nashville, TN, September 2012, pp. 1428-1434.

[35] J. A. Lopez-Salcedo, J.M. Parro-Jimenez, G. Seco-Granados , "Multipath detection metrics and attenuation analysis using a GPS snapshot receiver in harsh environments," Antennas and Propagation, 2009. EuCAP 2009. 3rd European Conference on, vol., no., pp.3692-3696, 23-27 March 2009.

[36] W. Jong-Hoon, B. Eissfeller, “A tuning method based on signal-to-noise power ratio for adaptive PLL and its relationship with equivalent noise bandwidth”, IEEE Comm. Letters, vol. 17, no. 2, February, pp. 393-396.

[37] W. Jong-Hoon, “A novel adaptive digital phase-lock-loop for modern digital GNSS receivers”, IEEE Comm. Letters, vol. 18, no. 1, January, pp. 46-49.

[38] X. Tang, G. Falco, E. Falletti, L. Lo Presti, “Theoretical analysis and tuning criteria of the Kalman filter-based tracking loop”, GPS Solutions, pp. 1-15, September.

[39] A. Pousinho, M. Toledo, T. Ferreira, J. A. López-Salcedo, S. Locubiche-Serra, G. Seco-Granados, M. A. Ribot, A. Jovanovic, C. Botteron, P.-A. Farine, R. Ioannides, “Adaptive Tracking Techniques in Non-Stationary Environments”, Proceedings of the 28th International Technical Meeting of the ION Satellite Division, ION GNSS+ 2015, Tampa, Florida, September 14-18, 2015.

[40] López-Salcedo, J. A., Capelle, Y., Toledo, M., Seco, G., Vicario, J. López, Kubrak, D., Monnerat, M., Mark, A., Jiménez, D., "DINGPOS: A Hybrid Indoor Navigation Platform for GPS and GALILEO," Proceedings of the 21st International Technical Meeting of the Satellite Division of The Institute of Navigation (ION GNSS 2008), Savannah, GA, September 2008, pp. 1780-1791.

[41] van Diggelen, F., “Method and Apparatus for Time-Free Processing of GPS Signals,” U.S. Patent 6,417,801, November 2000.

[42] G. Lachapelle, E. Cannon, R. Klukas, S. Singh, R. Watson, P. Boulton, A. Read, K. Jones, “Hardware Simulator Models and Methodologies for Controlled Indoor Performance Assessment of High Sensitivity AGPS Receiver” GNSS 2003, Graz, Austria.

[43] C. Ma, G. Jee, G. MacGougan, G. Lachapelle, S. Bloebaum, G. Cox, L. Garin, J. Shewfelt, "GPS Signal Degradation Modeling", ION GPS 2001, Salt Lake City.

[44] P. Boulton, A. Read, G. MacGougan, R. Klukas. E. Cannon, G. Lachapelle "Proposed Models and Methodologies for Verification Testing of AGPS-Equipped Cellular Mobile Phones in the Laboratory", Proceedings of ION GPS 2002, Portland, OR, 24–27. September, 200–212.

[45] Land Mobile Multipath Channel Model V3.0 by DLR http://www.dlr.de/kn/desktopdefault.aspx/tabid-8610/14830_read-36920/

[46] J.A. García-Molina, F. Zanier, M. Crisci, R. Prieto-Cerdeira, P. Giordano, A. Steingass, A. Hornbostel, "Land Mobile Multipath Channel Reduction Effects on a Real GNSS Receiver", NAVITEC 2010.